CLM-P724

UKAEA

Preprint

IDEAL MHD BALLOONING STABILITY IN THE VICINITY OF A SEPARATRIX

C. M. BISHOP
P. KIRBY
J. W. CONNOR
R. J. HASTIE
J. B. TAYLOR

CULHAM LABORATORY
Abingdon Oxfordshire

1984

CLM-P 724

IDEAL MHD BALLOONING STABILITY IN THE VICINITY OF A SEPARATRIX

C M Bishop, P Kirby, J W Connor

R J Hastie, J B Taylor

Culham Laboratory, Abingdon, Oxon OX14 3DB, UK

(Euratom/UKAEA Fusion Association)

Abstract

Using a model tokamak equilibrium we investigate the influence of a magnetic separatrix on the stability of the plasma against ideal MHD ballooning modes. We also give a physical interpretation of the results.

(Submitted for publication in Nuclear Fusion)

August 1984

I. Introduction

Auxiliary heated tokamaks generally exhibit a degradation of energy confinement time as the input power is raised. It has been conjectured[1] that this is due to local onset of ballooning instability where the pressure gradient exceeds the theoretical limit (calculated for circular magnetic surfaces). Recently[2,3,4] several tokamaks (Asdex, Doublet III and PDX) have operated in a new regime (the H-mode) in which degradation of confinement is less apparent. A significant feature of these machines is that the boundary of the plasma is defined by a magnetic separatrix, rather than by a material limiter. This is achieved by operating the tokamak with an axisymmetric (poloidal) divertor. The plasma may then exhibit either the L-mode, in which the usual degradation of confinement is observed, or the H-mode.

We are therefore led to investigate the ballooning stability limit for plasmas with a separatrix. To do this we consider a model tokamak equilibrium which allows us to investigate ballooning stability at various distances from the separatrix, and to examine the effect on marginal stability of changing the location (in poloidal angle) of the X-point. (We shall restrict our attention to the case of a single-null divertor.)

In section II we describe the model equilibrium and derive the corresponding ballooning equation. Results from a numerical solution of this equation are presented in section III, and we give some physical interpretation of these results in section IV.

II. Equilibrium and Ballooning Equation near a Separatrix

The theory of ballooning modes[5] allows us to calculate the stability of the plasma at a given flux surface in terms of equilibrium quantities given solely on that flux surface. It is therefore sufficient to consider a tokamak equilibrium near a single flux surface, and thereby avoid the complexity of having to construct a global equilibrium.

Consider the Grad-Shafranov equation for the poloidal flux function ψ :

$$X^2\nabla \cdot \frac{1}{X^2} \nabla\psi \quad = \quad -\left[X^2 p'(\psi) + II'(\psi)\right] \tag{1}$$

where X is the normal distance to the major axis, $p(\psi)$ is the plasma pressure, and $I(\psi)$ is the toroidal field function $\left(\vec{B}_\phi = I(\psi)\nabla\phi\right)$, and primes denote derivatives with respect to ψ . We introduce the coordinate system shown in Fig 1 in which ρ is the normal distance (in the poloidal plane) from the flux surface C , ℓ is the arc length measured along the surface, and ϕ is the toroidal angle. Following Mercier[6] we expand ψ , and the other equilibrium quantities, in powers of ρ around the flux surface (which we choose to be $\psi = 0$):

$$\psi \quad = \quad \psi_1\rho + \psi_2\rho^2 + \ldots$$

$$B_p \quad = \quad B_p^{(0)} + B_p^{(1)}\rho + \ldots$$

$$B_\phi = B_\phi^{(0)} + B_\phi^{(1)}\rho + \ldots$$

where $B_p = |\vec{B}_p|$ is the magnitude of the poloidal field $(\vec{B}_p = \nabla\psi \times \nabla\phi)$. From Fig 1 we also have

$$X = X_0 h_0 + \rho \sin u$$

$$h_0 = 1 + \frac{1}{X_0} \int_0^\ell \cos u \, d\ell ,$$

where $u(\ell)$ is the angle between the local tangent to the curve and the X-axis. We can calculate $u(\ell)$ from

$$u(\ell) = - \int^\ell \frac{d\ell'}{R(\ell')}$$

where $R(\ell)$ is the local radius of curvature of the surface in the poloidal plane. Substituting into Eq (1) and equating powers of ρ we obtain the following equilibrium relations

$$\psi_1 = -B_p X_0 h_0 \quad (2)$$

$$\psi_2 = -\left(\sin u + \frac{X_0 h_0}{R}\right) \frac{B_p^{(0)}}{2} - \frac{X_0{}^2 h_0{}^2 p'}{2} - \frac{II'}{2} \quad (3)$$

$$B_p^2 = B_p^{(0)2} \left[1 + 2\rho \left\{\frac{1}{R} + \frac{p' X_0 h_0}{B_p^{(0)}} + \frac{II'}{h_0 X_0 B_p^{(0)}}\right\}\right] \quad (4)$$

$$B_\phi^2 = \frac{I^2}{X_0{}^2 h_0{}^2}\left[1 - \frac{2\rho}{X_0 h_0}\left\{\frac{I'}{I} X_0{}^2 h_0{}^2 B_p^{(0)} + \sin u\right\}\right] \quad . \tag{5}$$

The equilibrium is specified by prescribing the shape of the surface (which determines $R(\ell)$ and $u(\ell)$) and the poloidal field $B_p^{(0)}(\ell)$ on the surface. These quantities can be chosen arbitrarily, and in doing so it must be assumed that a corresponding global equilibrium exists. (This is not guaranteed, however, since a continuation of the solution into the magnetic axis could yield a singularity.)

For simplicity we choose surfaces whose shape and poloidal field distribution correspond to those generated by the field of a pair of parallel wires carrying equal currents[7] (this field structure posesses a separatrix, with an X-point midway between the wires). Note that we are using this straight system only to determine the functions $R(\ell)$, $u(\ell)$ and $B_p^{(0)}(\ell)$, and that our equilibrium is calculated in toroidal geometry. We shall consider only those surfaces lying inside the separatrix. These surfaces are labelled by a parameter k such that as $k \to 0$ the surface becomes circular (and $B_p^{(0)}$ becomes independent of ℓ). In this limit our equilibrium model and ballooning equation reduce to those of the "s-α" model[8]. As $k \to 1$ the shape of the surface approaches that of a separatrix.

In polar coordinates (r,θ) the shape of the surface is specified implicitly by

$$k^2 = \frac{r^2}{r_0^2}\left[\sqrt{(1 + k)} - 1\right]^2 \{4 + \frac{r^2}{r_0^2}\left[\sqrt{(1 + k)} - 1\right]^2$$

$$- 4\frac{r}{r_0}\cos(\theta - \gamma)\left[\sqrt{(1 + k)} - 1\right]\} \tag{6}$$

and the poloidal field is given by

$$\left\{\frac{B_p^{(0)}}{B_0}\right\}^2 = \frac{1 + \frac{r^2}{r_0^2}\left[\sqrt{(1 + k)} - 1\right]^2 - 2\frac{r}{r_0}\left[\sqrt{(1 + k)} - 1\right]\cos(\theta - \gamma)}{(1 + k)} . \tag{7}$$

Eqs (6) and (7) are normalised so that at the point on the surface directly opposite the X-point, both r and $B_p^{(0)}$ are independent of k, and are given by $r = r_0$ and $B_p^{(0)} = B_0$ respectively. Successive values of k then generate equilibria having roughly the same toroidal current. Fig 2 shows plots of the surfaces for various k-values, and also defines the angle γ (the poloidal location of the X-point) used in Eqs (6) and (7).

We can calculate the function $R(\theta)$ from

$$R(\theta) = \frac{\left[r^2 + \left(\frac{dr}{d\theta}\right)^2\right]^{3/2}}{\left[r^2 + 2\left(\frac{dr}{d\theta}\right)^2 - r\frac{d^2r}{d\theta^2}\right]} .$$

To investigate the ballooning stability of our equilibrium we must solve the ballooning equation which, for marginal stability, can be written

$$\vec{B}\cdot\nabla \left\{\frac{|\nabla S|^2}{B^2}\,\vec{B}\cdot\nabla F\right\} + 2p' \,\frac{(\vec{B}\times\nabla S)}{B^2}\cdot\nabla_{\perp}(p + B^2/2)F \;=\; 0 \qquad (8)$$

where F and S are quantities which appear in the eikonal form for the plasma displacement $\xi = Fe^{inS}$ [5]. Using the relation $\vec{B}\cdot\nabla S = 0$ we can construct S as an expansion in powers of ρ to give

$$S = \phi - I\int_{\ell_0}^{\ell} \frac{d\ell}{X_0^2 h_0^2 B_p^{(0)}} + \rho B_p^{(0)} I h_0 \int_{\ell_0}^{\ell} \frac{d\ell}{B_p^{(0)} h_0^3 X_0^2}\left[\frac{B_p^{(0)} X_0 h_0 I'}{I} + \frac{2\sin u}{X_0 h_0}\right. \qquad (9)$$

$$\left. + \frac{2}{R} + \frac{X_0 h_0}{B_p^{(0)}}\,p' + \frac{II'}{B_p^{(0)} X_0 h_0}\right] .$$

Note that the ballooning mode formalism introduces an undetermined parameter ℓ_0 . In solving Eq (8), ℓ_0 must be given the value which gives rise to the most unstable mode.

We now use the equilibrium relations (4) and (5), together with Eqs (8) and (9), to derive the required ballooning equation. After making an expansion in powers of the inverse aspect ratio $\varepsilon \sim r_0/X_0$, and keeping only the leading order terms, we obtain

$$B_p^{(0)} \frac{d}{d\ell} \left[\left\{ \frac{1}{B_p^{(0)2}} + P^2(\ell) \right\} B_p^{(0)} \frac{dF}{d\ell} \right] - \frac{\alpha B_0}{r_0^2} \left\{ \frac{\sin u}{B_p^{(0)}} + \cos u \, P(\ell) \right\} F = 0 \tag{10}$$

where

$$P(\ell) = B_p^{(0)} \int_{\ell_0}^{\ell} \frac{d\ell}{B_p^{(0)3}} \left\{ \frac{\sigma B_0}{r_0} + \frac{2B_p^{(0)}}{R} - \frac{\alpha B_0}{r_0^2} \int_0^{\ell} \cos u \, d\ell \right\} \tag{11}$$

and we have introduced the parameters

$$\sigma = \left(p' + \frac{II'}{X_0^2} \right) \frac{X_0 r_0}{B_0} \tag{12}$$

$$\alpha = - \frac{2p' r_0^2}{B_0} . \tag{13}$$

As a consequence of the ballooning transformation, the arc length variable ℓ in Eq (10) lies on $[-\infty , \infty]$. Note that as $k \rightarrow 0$ our definition of α becomes identical to the definition $\alpha = -2X_0(dp/dr)q^2/B^2$ introduced in [8].

Eq (10) determines the critical pressure gradient as a function of σ and k. The quantity σ is proportional to the toroidal current density. Since the outer regions of the plasma are relatively cool, and therefore resistive, the current density near the separatrix will be small. We therefore set $\sigma = 0$, and determine $\alpha(k)$. To some extent

$\alpha(k)$ replaces $\alpha(s)$ in earlier work (where s is a parameter describing global shear), but note that although k controls the shear it does so by changing the shape of the flux surfaces, rather than by changing the plasma current. We can define a global shear s to be

$$s = \frac{X_0 r_0 B_0}{q} \frac{dq}{d\psi}$$

where $q(\psi)$ is the safety factor. Again, for circular flux surfaces this coincides with the definition $s = (r/q)dq/dr$ of [8]. To leading order in the inverse aspect ratio we have

$$s = \frac{r_0 B_0 \oint \frac{d\ell}{B_p^{(0)3}} \left\{\frac{\sigma B_0}{r_0} + \frac{2B_p}{R} - \frac{\alpha B_0}{r_0^2} \int_0^{\ell} \cos u \, d\ell\right\}}{\oint \frac{d\ell}{B_p^{(0)}}} . \quad (14)$$

III. Results

The two-point boundary-value problem represented by Eq (10) was solved using a finite difference scheme based on the Lentini-Pereyra deferred correction algorithm[9]. We demonstrate the effect of the separatrix on ballooning stability by plotting graphs of α against k for various values of the angle γ. As $k \to 1$ the shape of the magnetic surface, and the distribution of poloidal field on the surface, approach those of a separatrix. In Figs 3 to 5 we show the results for $\gamma = 3\pi/4$, $\pi/2$ and 0. In each case there are two regions of stability separated by an unstable region. These stable regions correspond to the first and second stability regions of the s-α model. Fig 3, for $\gamma = 3\pi/4$, corresponds to the single null divertor configuration in PDX. In this case the marginal α shows a moderate dependence on the shaping parameter k. The results shown in Fig 4 for $\gamma = \pi/2$, corresponding to the divertor configuration in ASDEX, show a similar behaviour for the marginal α. This contrasts with the case of $\gamma = 0$, shown in Fig 5, which corresponds to an X-point on the outside of the torus as in the new large tokamak JT-60. In this case the critical α falls markedly as $k \to 1$.

As these results suggest, the location of the X-point plays an important role in determining the stability to ballooning modes. This is confirmed in Fig 6 which shows the first stability boundary for various values of γ ‡.

---

‡ Studies of ballooning stability near a separatrix have also been carried out by R W Moore, L C Bernard and M S Chu (private communication). They define an α-like quantity by

$$\alpha = -\frac{p'V'}{2\pi^2}\left(\frac{V}{2\pi^2 X_0}\right)^{1/2}$$

where $V(\psi)$ is the volume enclosed by the flux surface. Since $V'(\psi)$ increases as $k \to 1$ they obtain larger values of α near the separatrix. When our answers are expressed in terms of this definition of α we find results which are in broad agreement.

IV Physical Interpretation and Conclusions

There are two aspects of a magnetic separatrix which we might expect to influence the ballooning stability limit. The first is the global shear of the magnetic field which becomes large as we approach the separatrix. This can be seen from Fig 7 which shows the global shear s corresponding to the first stability boundary of Fig 3. In general we expect this strong shear to exert a stabilising influence. The second effect of the separatrix arises because the poloidal field becomes very small in the neighbourhood of the X-point. Consequently, the "connection length" along a field line between the inside and outside of the torus is increased and the field line "lingers" for much of its length in the vicinity of the X-point. The lengthening of the field line will generally be expected to weaken the stability while the lingering effect will be expected to improve stability if it occurs in the good curvature region (the inside of the torus) or to impair stability if the lingering is in the bad curvature region (the outside of the torus).

It is clear from our results that the strong shear as $k \to 1$, shown in Fig 7, is not the dominant factor in determining stability to ballooning modes. Instead the fact that the critical α depends strongly on the poloidal location of the X-point, as shown in Fig 6, suggests that it is the field line lingering which is the dominant influence. This interpretation is supported by an examination of the marginally stable eigenfunctions. Fig 8 shows the eigenfunction for $\gamma = 3\pi/4$, $k = 0.99$. The X-point is at $\theta = \frac{3\pi}{4} \pm n2\pi$, $n = 0,1,2,\ldots,$ in this figure, and we see that the eigenfunction is localised on the outside of the torus and falls to zero at the X-point, so minimising the stabilising effect of field line lingering in the region of good curvature. By contrast the eigenfunction for $\gamma = 0$, $k = 0.99$, shown in Fig 9, is spread out in poloidal angle. It makes many poloidal circuits and on each circuit exploits the field line lingering in the region of bad curvature.

Since it is field line lingering near the X-point, rather than global shear, which controls ballooning stability near a separatrix, the greatest stability against ideal ballooning modes will be obtained with the X-point on the inside of the tokamak.

References

[1] CONNOR, J W, TAYLOR, J B, TURNER, M F, Nucl Fusion 24 (1984) 642

[2] OHYABO, N, et al, to appear in the proceedings of the IEEE International Conference on Plasma Science, San Diego, CAl, May 1983, and NAGAMI, M, et al, GA-A17056, May 1983

[3] KAYE, S M, et al, Syposium on Energy Removal and Particle Control in Toroidal Fusion Devices, July 1983, Princeton

[4] WAGNER, F, et al, Phys Rev Lett 49 (1982) 1408

[5] CONNOR, J W, HASTIE, R J, TAYLOR, J B, Proc R Soc Lond A365 (1979) 1

[6] MERCIER, C, LUC, N, in "MHD Approach to Confinement in Toroidal Systems" EUR 5127e (1974) 140

[7] HOBBS, G D, TAYLOR J B, Culham Lab Report CLM-R95 (1968)

[8] CONNOR, J W, HASTIE, R J, TAYLOR, J B, Phys Rev Lett 40 (1978) 396

[9] LENTINI, M, PEREYRA, V, S.I.A.M. J Numer Anal 14 (1977) 91

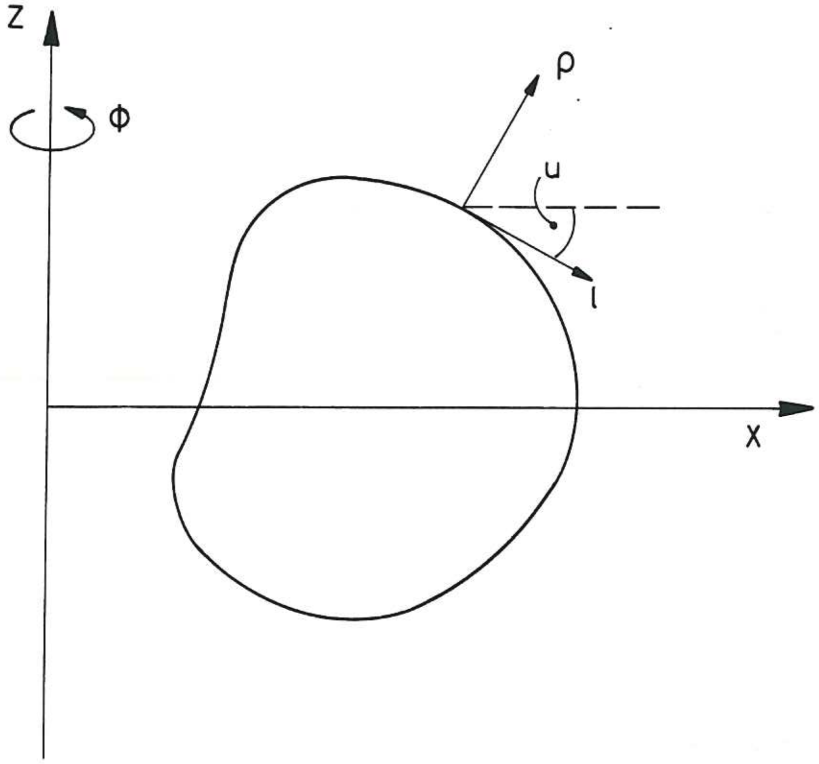

Fig. 1 Co-ordinate system used for the construction of the equilibrium.

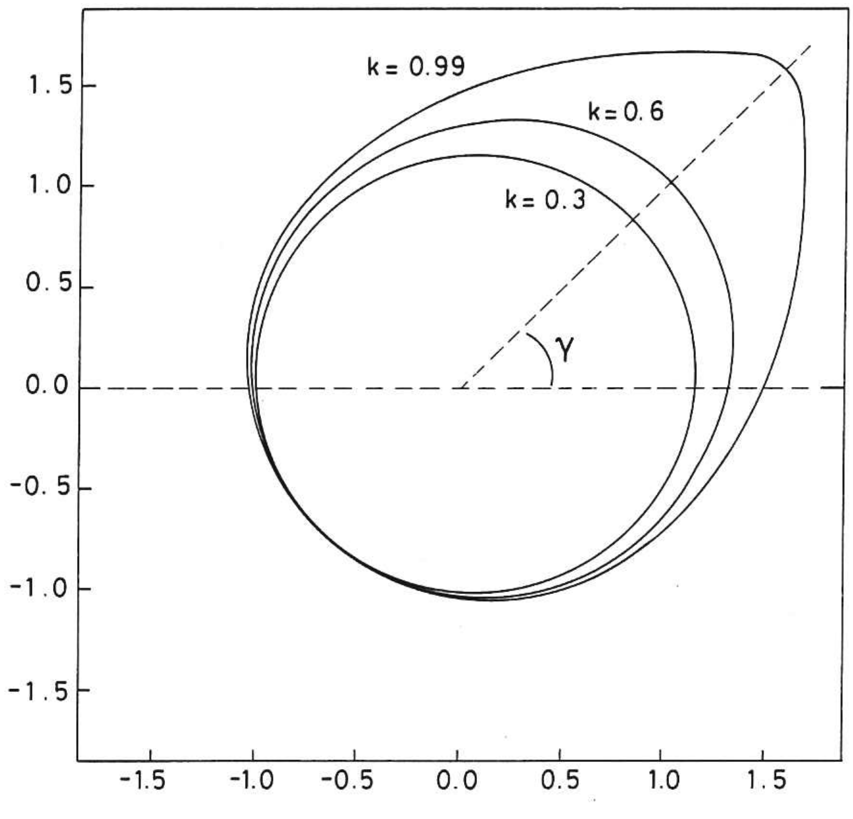

Fig. 2 Plots of the magnetic surfaces corresponding to various values of k.

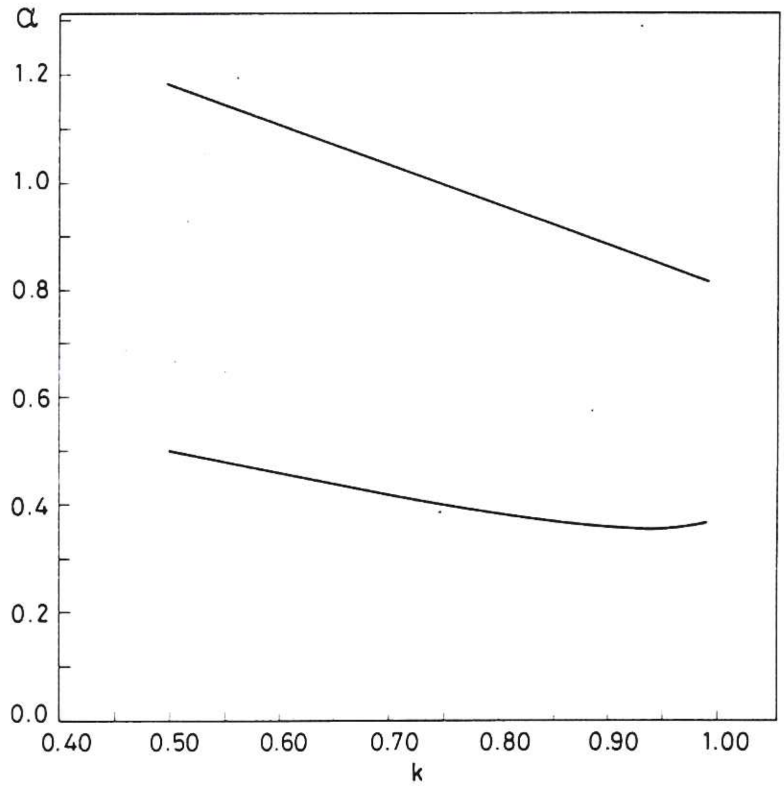

Fig.3 Dependence on k of the marginally stable α, for $\gamma = 3\pi/4$.

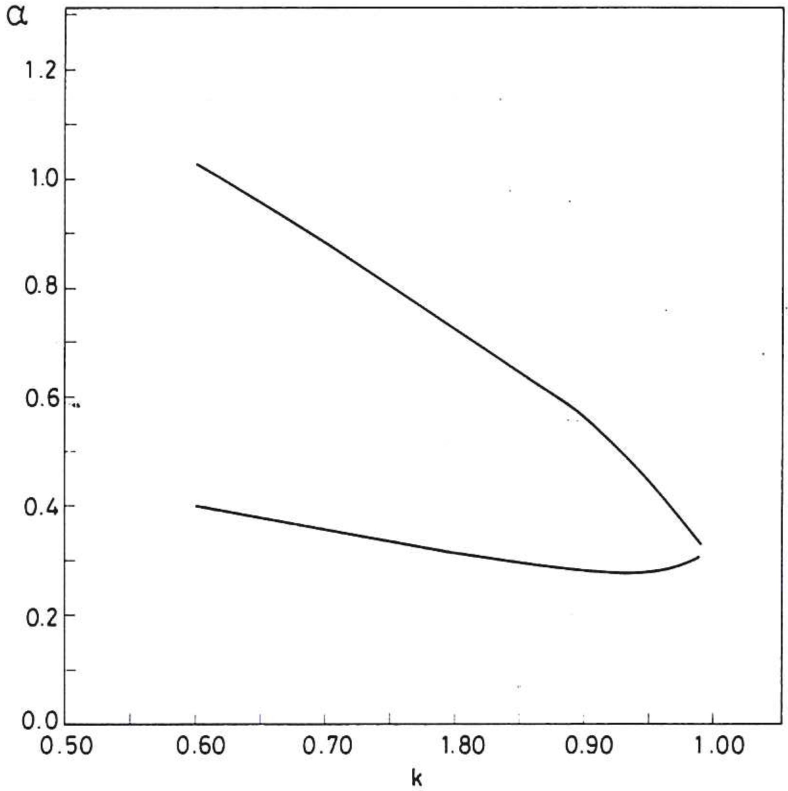

Fig.4 Dependence on k of the marginally stable α, for $\gamma = \pi/2$.

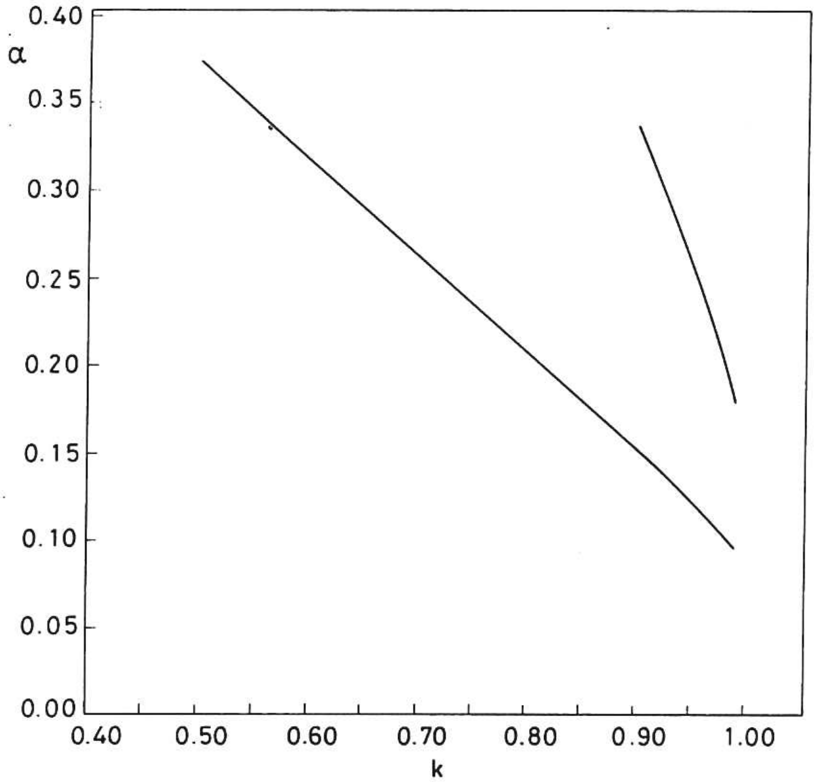

Fig.5 Dependence on k of the marginally stable α, for $\gamma = 0$.

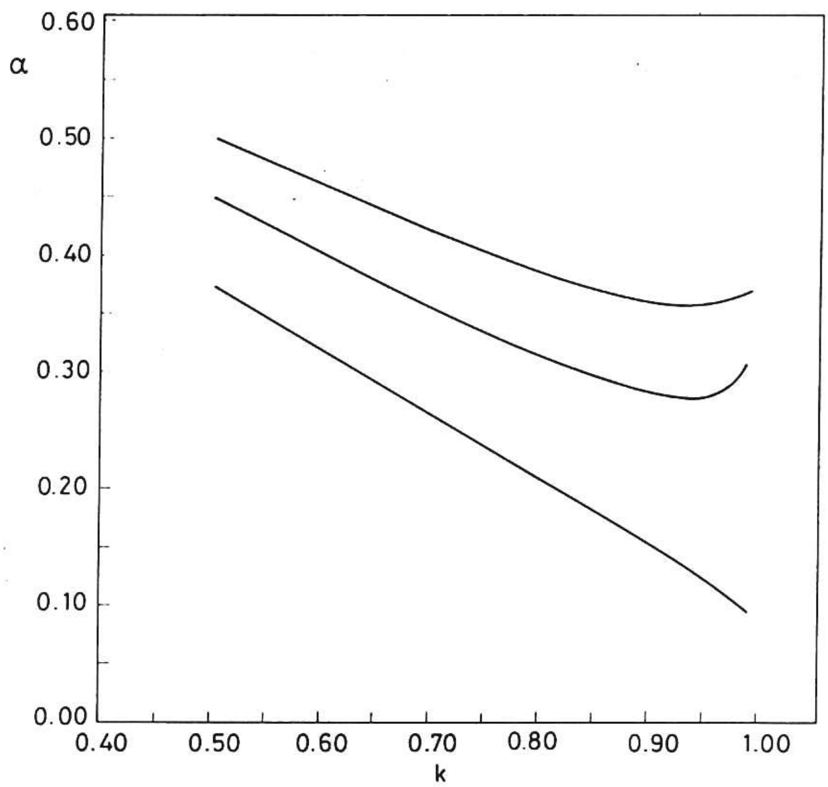

Fig.6 Comparison of the first stability boundaries for various values of γ.

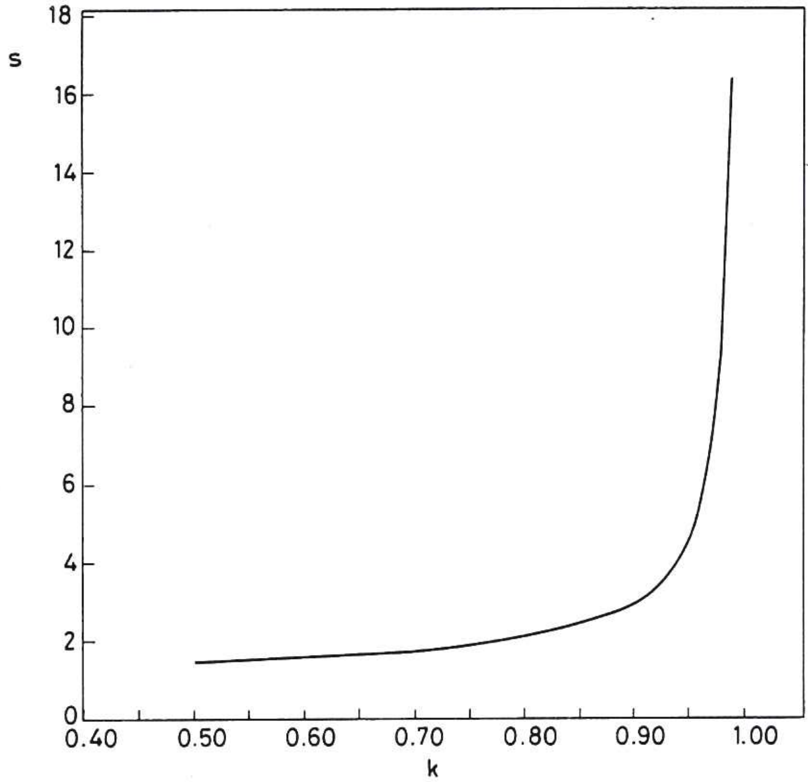

Fig. 7 Global shear s as a function of k for the first stability boundary of Fig. 3.

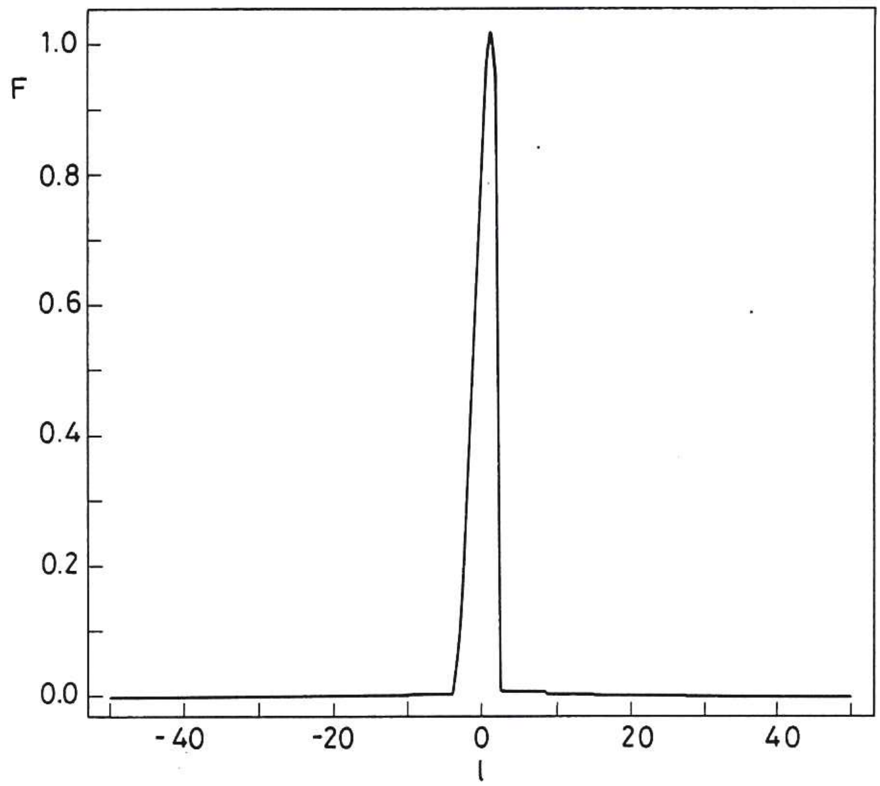

Fig. 8 Eigenfunction at the first stability boundary for $\gamma = 3\pi/2$, k = 0.99.

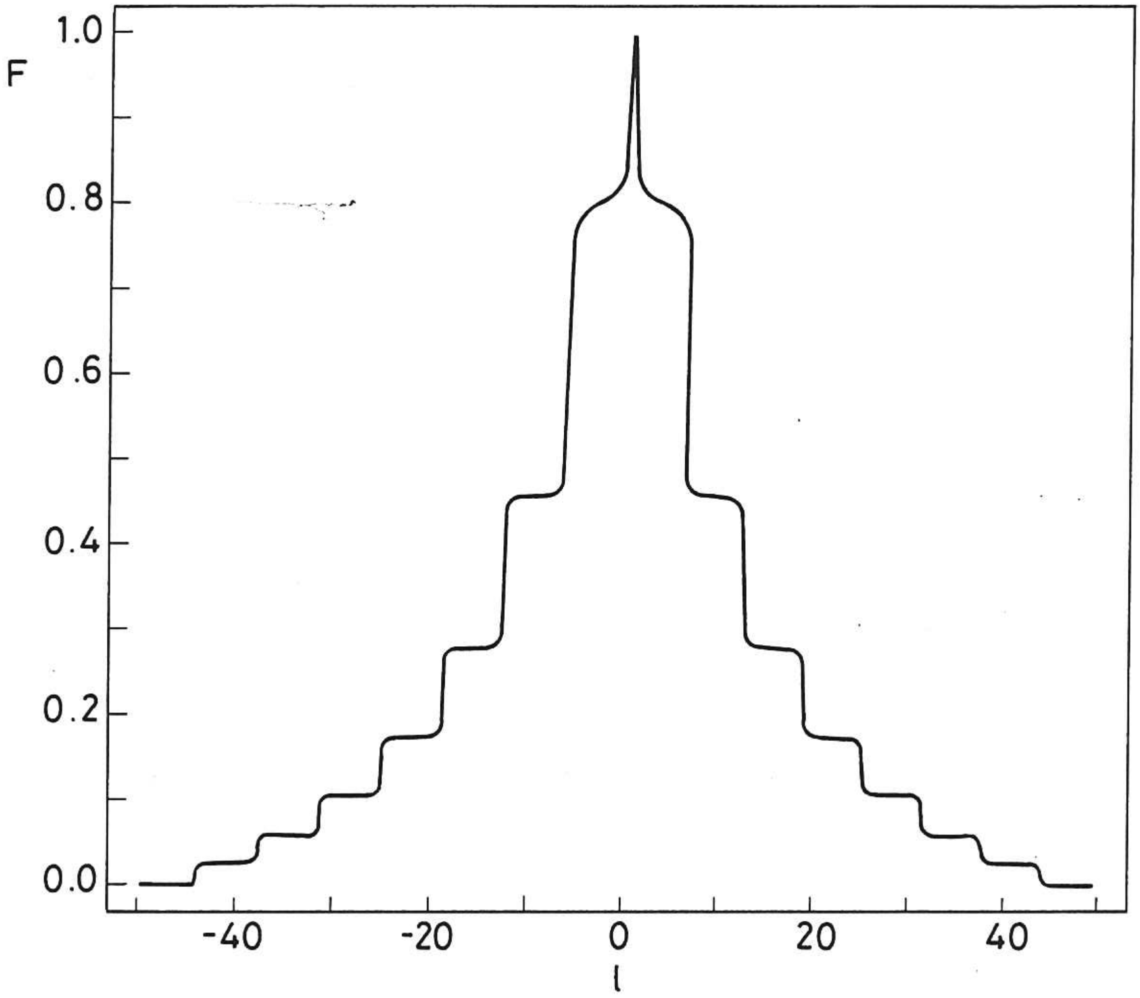

Fig.9 Eigenfunction at the first stability boundary for $\gamma = 0$, $k = 0.99$.